European Journal of Geography

Volume 11, Issue 4, pp. 144 - 156

Article Info:
Accepted: 16/12/2020
Corresponding Author: *triantafyllos.falaras@gmail.com
https://doi.org/10.48088/ejg.t.fal.11.4.144.156

Special Issue: *"Selected Papers from 12th International Conference of the Hellenic Geographical Society (ICHGS): Innovative Geographies II, 2019"*

Multitemporal observation of Karla reservoir in Thessaly Greece utilizing SAR and optical remotely sensing imagery

Triantafyllos **FALARAS**[1*], Maria **KOILAKOU**[1], Leonidas **TSOUKALAS**[1]

[1] *Harokopio University, Greece*

Keywords:
Remote Sensing,
Inland water Mapping,
Optical Imagery,
SAR Imagery,
Lake Karla,
ICHGS-2019

Abstract

Wetlands constitute areas with significant value and service offerings both in anthropogenic and natural environments. Taking into consideration the importance of studying wetland ecosystems and their changes, the aim of this paper is the observation of Lake Karla's reservoir fluctuation, since its reconstitution in 2010. For this reason, annual and seasonal fluctuations of the reservoir were estimated, utilizing remote sensing Synthetic Aperture Radar (SAR) (Sentinel 1) and optical (Sentinel 2) imagery, as well as Landsat 5 imagery. For SAR imagery an image segmentation method with a dynamic threshold operator based on mean values is utilized, while for optical imagery the Normalized Difference Water Index (NDWI) is applied. The findings reveal changes in Karla's reservoir, with its acreage being continually increased on average on an annual basis. Meanwhile, on a seasonal basis, the results indicate some variations in the reservoir, due to precipitation and irrigation purposes.

The publication of the European Journal of Geography (EJG) is based on the European Association of Geographers' goal to make European Geography a worldwide reference and standard. Thus, the scope of the EJG is to publish original and innovative papers that will substantially improve, in a theoretical, conceptual or empirical way the quality of research, learning, teaching and applying geography, as well as in promoting the significance of geography as a discipline. Submissions are encouraged to have a European dimension. The European Journal of Geography is a peer-reviewed open access journal and is published quarterly.

1. INTRODUCTION

Global environmental issues such as climate change and anthropogenic interventions like pollution, land use changes and over-exploitation of natural resources are putting pressure on ecosystems. In this way, all modern societies are about to face a "green" challenge: the biodiversity preservation of all aquatic ecosystems. As a constituent aquatic ecosystems, the lakes as well as their surrounding areas, constitute extremely vital and dynamic biodiversity sites that needs monitoring, conservation, and protection due to its physical, economic, social and cultural values (Dellepiane et. al., 2004; Climate Change Impacts Study Committee, 2011; Paes et. al., 2015; Zormpas et al., 2017).

In particular, knowledge derived from the study of the fluctuations as well as the behavior of inland water bodies in general is an important tool in a variety of research fields such as space planning, management, and sustainable development, as well as environmental management of water resources (Dellepiane et. al., 2004; Liu & Jezek, 2004; Sheng et. al., 2012). The extraction of information about area measurements in a water body can occur either by field research, optical interpretation (using high resolution aerial photography) or by remote sensing (RS) processing of optical/multispectral and Synthetic Aperture Radar (SAR) images, each of which is characterized of advantages and disadvantages (Pradhan et. al., 2018).

More specifically, regarding SAR sensors, their broad spatial coverage, their high spatial resolution, their ability to acquire imagery regardless of the weather conditions and the time of the day, make their data a reliable source of information in the environmental research (Brisco, 2015; Parcharidis, 2015). As for the disadvantages, the methods and techniques of discerning water bodies with SAR imagery, are requiring computing hardware of high performance and the user's advanced skills for manual modifications (Paes et. al. 2015, Liu et. al., 2016). More specifically, the manual modifications in many cases include the delineation between the land surface and water, using thresholding (Liu, 2016; Prasad, Garg and Thakur, 2018).

On the other hand, optical imagery is also widely used in inland waterbody mapping with plenty of methods being developed. The methods used are discerned to those which use one spectral band and the other which use multiple spectral bands (McFeeters, 1996; Χυ, 2006). One of these methods the Normalized Difference Water Index (NDWI) of McFeeters (1996), which is applied in most of the cases in the bibliography and it is also applied to our study. The difficulties related to the use of optical imagery, are the cloud coverage and the time of image acquisition in one area (Parcharidis, 2015).

The aim of this study is the observation of lake Karla's reservoir fluctuation since its reconstitution, with the use of remote RS techniques. The usage of SAR and optical imagery, with their respective methods, aims to monitor the variations of an inland waterbody reservoir. Furthermore, the contribution of different RS data is compared in order to highlight the potential of each sensor.

2. STUDY AREA

The basin of lake Karla is located in the southeastern Thessaly in Central Greece, between the administrative boundaries of Magnesia and Larissa prefectures, near Volos (Fig. 1). It is an elongated, shallow and relatively enclosed area of about 1.660 Km^2 without a physical surface hydraulic communication with the sea, which reduced to 1171 Km^2 after the drainage projects (Sidiropoulos, 2014). The main source of that basin's water supply is the surface network of Pinios canals and the aquifer (Xenarios et. al., 2016). The area of the lake before the drainage procedures exhibit fluctuations from 40 to 108 Km^2, due to the Pinios river floods phenomena (Zisou & Psilovikos, 2012). As a whole, the geomorphological evolution of the basin is a result of climatic, lithological, tectonic and geomorphic conditions and processes during the Quaternary period (Gaki-Papanastasiou, 2011). More specifically, the Karla basin is a tectonic sink which due to its formulation with sandy lake deposits and coarse-grained sediments, has led to a high hydro permeable background (Gerakis, 1992). As a result of the basin's terrain, about 60% is characterized as agricultural land (Sidiropoulos, 2014). More analytically, according to Corine Land Cover 2018, most of the area is covered by permanently irrigated and non-irrigated arable land, followed by hardwood vegetation and pastures. The climate of Karla's wider area is characterized as Mediterranean with dry and hot summers and cold and humid winters (Xenarios et. al., 2016).

Lake Karla reservoir was drained in 1962 by the Greek State due to the need for flood control, to combat malaria and to provide a living to the locals by creating more land for agriculture. After the accomplishment of this project, it was proved that its consequences were more severe than its benefits. The drainage caused the incapacity of water supply in surrounding areas such as the fall of groundwater level, impacts in biodiversity with fauna and flora being negatively affected and last but not least, impacts in the microclimate of the area. For this reason, after the evaluation of these negative effects in the late 1990's the reconstitution of the reservoir of 38 Km^2 was conceived and started. Its purpose was to aid the irrigation of the area, its flood protection and the restoration of the ecosystem's balance. With the proper infrastructure constructed in the December of 2010, the pumping of water from Pinios to the new Lake Karla reservoir was started. (Ministry for the Environment, Spatial Planning and Public Works, 2008; Sidiropoulos, 2014; Water Resources and Environment of Thessaly, 2019)

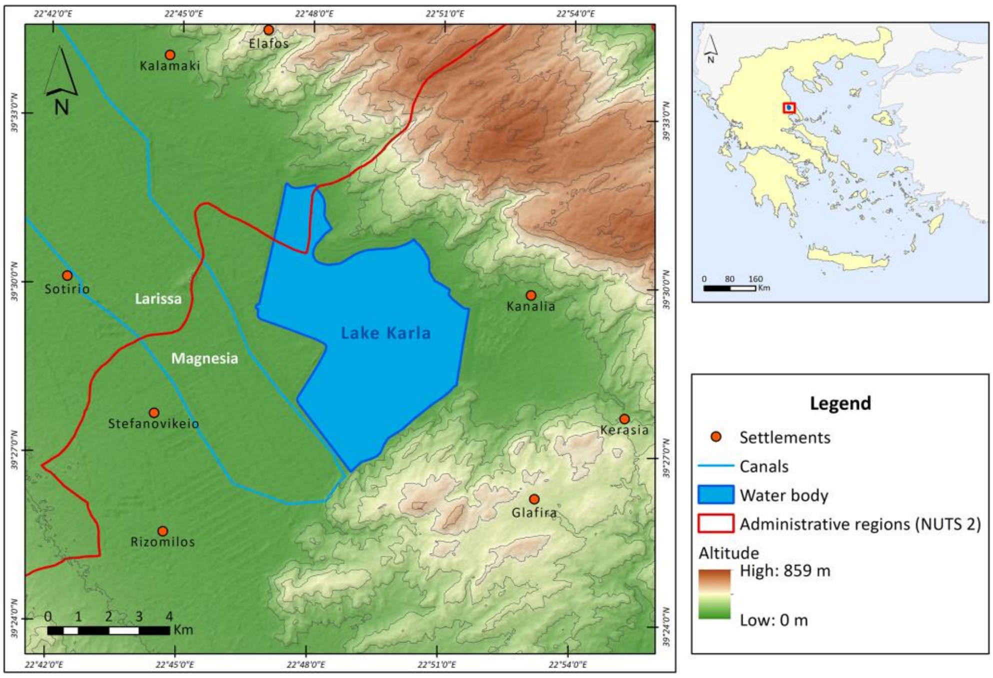

Figure 1. Study area.

3. DATA AND METHODOLOGY

3.1 Data

The dataset used for the extraction of the Lake Karla's surface consists of both Sentinel 1 and 2 satellite images, as well as two Landsat 5 images (See Table 1). For the estimation of:

- the annual changes, a Landsat 5 optical image was used for the 2010, as well as 4 Sentinel 1 images, one per year, for the period 2014-2018.
- the relative two-month change for 2017 was exploited 6 Sentinel 1 images
- the monthly comparison for 2018, 12 Sentinel 1 and 10 Sentinel 2 images (January-October) were used.

More specifically these data are:

(i) Sentinel 1 SAR imagery. The products used are Ground Range Detected products (GRD) Interferometric Wide swath (IW) of Ascending and Descending acquisition orbit and Vertical Vertical (VV) polarization. GRD products are georeferenced, focused and assigned with terrain geometry and their spatial resolution is 20 m X 22 m (10 m X 10 m imagery resolution). (European Space Agency, 2012; European Space Agency 2019)

(ii) Sentinel 2 optical imagery. The products used are Level-1C (L1C) which are georeferenced and radiometrically corrected. Its spectral bands have a spatial resolution of 10 m, 20 m, and 60 m. (European Space Agency, 2012; European Space Agency, 2015; European Space Agency, 2019)
Sentinel imagery is available from Copernicus Open Access Hub platform (URL: https://scihub.copernicus.eu/)

(iii) Landsat 5 TM optical imagery. These products were downloaded from USGS Earth Explorer platform (URL: https://earthexplorer.usgs.gov/). They are geometrically corrected. The Thematic Mapper (TM) six out of seven bands have a spatial resolution of 30 m X 30 m. (USGS, 2019)

(iv) The meteorological data were downloaded from Meteo.gr (URL: http://meteosearch.meteo.gr/) of National Observatory of Athens. These data are taken from the nearest meteorological station of Agia, Larissa in 167m altitude.

Table 1. Remotely Sensed imagery.

SAR Imagery		Optical Imagery	
Sentinel 1 GRD IW		Sentinel 2 L1C IW	Landsat 5 TM
24/10/2014 S1A Asc	24/1/2018 S1B Desc	19/1/2018 S2B Desc	5/7/2008
21/10/2015 S1A Asc	5/2/2018 S1B Desc	8/2/2018 S2B Desc	31/10/2010
25/10/2016 S1A Asc	25/3/2018 S1B Desc	30/3/2018 S2B Desc	
22/2/2017 S1A Asc	24/4/2018 S1A Desc	24/4/2018 S2A Desc	
24/4/2017 S1A Asc	18/5/2018 S1B Desc	19/5/2018 S2B Desc	
22/6/2017 S1B Asc	23/6/2018 S1A Desc	23/6/2018 S2A Desc	
27/8/2017 S1B Desc	29/7/2018 S1A Desc	28/7/2018 S2B Desc	
26/10/2017 S1B Asc	22/8/2018 S1A Desc	22/8/2018 S2A Desc	

25/12/2017 S1B Asc	21/9/2018 S1B Desc	21/9/2018 S2A Desc	
	27/10/2018 S1B Desc	26/10/2018 S2B Desc	
	20/11/2018 S1B Desc		
	20/12/2018 S1A Desc		
Asc: Ascending / Desc: Descending *S1A: Sentinel 1A / S1B: Sentinel 1B | S2A: Sentinel 2A / S2B: Sentinel 2B* *Source: Copernicus Open Access Hub*			*Source: USGS Earth Explorer*

Supplemental to the above RS data, for the presentation of the results, were also used the data shown in Table 2.

Table 2. Additional data and their source.

Data	Type	Source
Aster GDEM	Raster (~30 m)	NASA Earthdata
Settlements	Vector	Geoportal of Special Secretariat for Water
Administrative prefectures	Vector	Geodata.gov.gr
Rivers	Vector	Geoportal of Special Secretariat for Water
Lakes	Vector	Geoportal of Special Secretariat for Water

3.2 Methodology

The resolution of SAR images is 10 m X 10 m and for this reason, optical images are resampled with the bicubic method to match this resolution. All the imagery used was subsetted before the processing so as to focus on the study area and to maximize the speed of processing. Also, the last part of the processing in both methodologies is common and includes the import of the RS products in a GIS environment, their reclassification, their raster to vector polygon conversion form which is retained only the surface of the lake and lastly the area calculation. The projection system used and assigned to the data is the WGS 1984 UTM Zone 34N which is proper for the study area. Regarding processing, it took place in the open software of European Space Agency STEP platform SNAP 6.0, while the visualizations and measurements were done in the commercial software ArcGIS 10.4 of ESRI.

3.2.1 SAR Imagery

In SAR imagery, it is important to mention the roughness of water surfaces before analyzing the methodology. More specifically, in SAR C-band the water surfaces usually have very low backscattering values in comparison with other surfaces. Due to this reason, water bodies are looking dark because they are behaving like mirrors. (Westerhoff et. al., 2013; Liu, 2016; Pham-Duc, Prigent, & Aires, 2017)

Following the subset of the images, the next step is their Calibration, which assigns the radar backscatter values of the scene to the pixels, creating a new sigma-nought image format, useful for quantitative purposes. After that Linear to db command is implemented, and the existed pixel values are converted to decibel (dB) (SNAP, 2019). SAR images inherent "noise" called speckle, caused by random constructive and destructive interference of the de-phased but coherent return waves scatter by the elementary scatters within each resolution cell. Keeping in mind that speckles degrade the quality of the image and make feature interpretation more difficult, in our case is applied the Lee filter 5x5 (Lee et. al., 1994). The Lee filter is designed to eliminate speckle "noise" while retaining edges and point features in radar imagery (Yu & Acton, 2002). The images are then geometrically corrected using the Range Doppler Terrain Correction Operator, where the geometric correction is based on the SRTM 3sec digital elevation model used by the software. At this point of the processing, follows calculation of the threshold which is calculated using each image histogram, in order to separate the land and water, following the below formula:

$$T = \frac{\mu s + \mu I}{2} \quad \textbf{[1]}$$

Where: T= Threshold value, μs: Mean value of water class distribution, μI= Mean value of land class distribution (Bioresita & Hayati, 2016). Then, the Band Math tool is used for the separation of the land and water through the following mathematical operation (Equation 2).

$$255^* \text{ (sigma0\_VV} < \mathrm{T}) \quad \textbf{[2]}$$

Sigma0_VV is the image in which the above mathematical operation is applied, while T is the threshold at which the two values are divided. Since the above procedures resulted in binary images, in which water is separated by land, it is now possible to process them in ArcGIS as mentioned before.

3.2.2 Optical Imagery

Analyzing the methodology utilizing optical imagery, after the preprocessing mentioned before, the NDWI (Normalized Difference Water Index) index was applied. NDWI utilizes the spectral bands of visible Green and Near Infrared (NIR), which are used to make a distinction between land and water according to the Equation 3. More analytically, this index with the use of visible Green band increases the typical reflectance of water while the Near Infrared band decreases its low reflectance in water. In other words, it takes advantage of the high reflectance of soil and vegetation in Near-Infrared having values ranging from -1 to 1. (McFeeters, 1996)

$$NDWI = \frac{(Green - NIR)}{(Green + NIR)} \quad \textbf{[3]}$$

Then, in the new NDWI image in order to distinguish clearly the water and land surface, a thresholding via Band Maths was applied (Equation 4). The NDWI values bigger than 0.3 represent the water while values smaller than 0.3 represent the land surface (McFeeters, 2013). After the reprojection of the results in the desired projection system, they were exported as GeoTIFF and the final processes mentioned before took place.

$$Waterbody = 255 * (NDWI > 0.3) \quad \textbf{[4]}$$

4. RESULTS

The results of all the above procedures led to the below figures, concerning the area occupied by Lake Karla, annually, seasonally and monthly for the time period from 2010 to 2018.

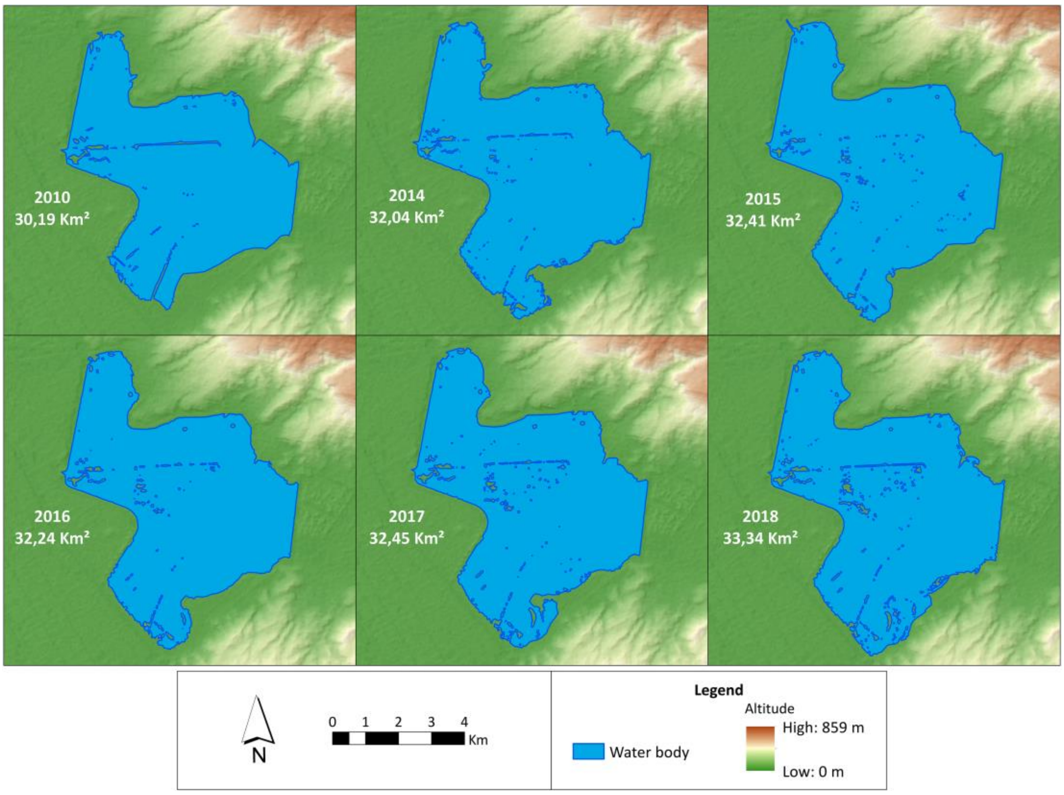

Figure 2. Annual area of water body change 2010-2018 per year.

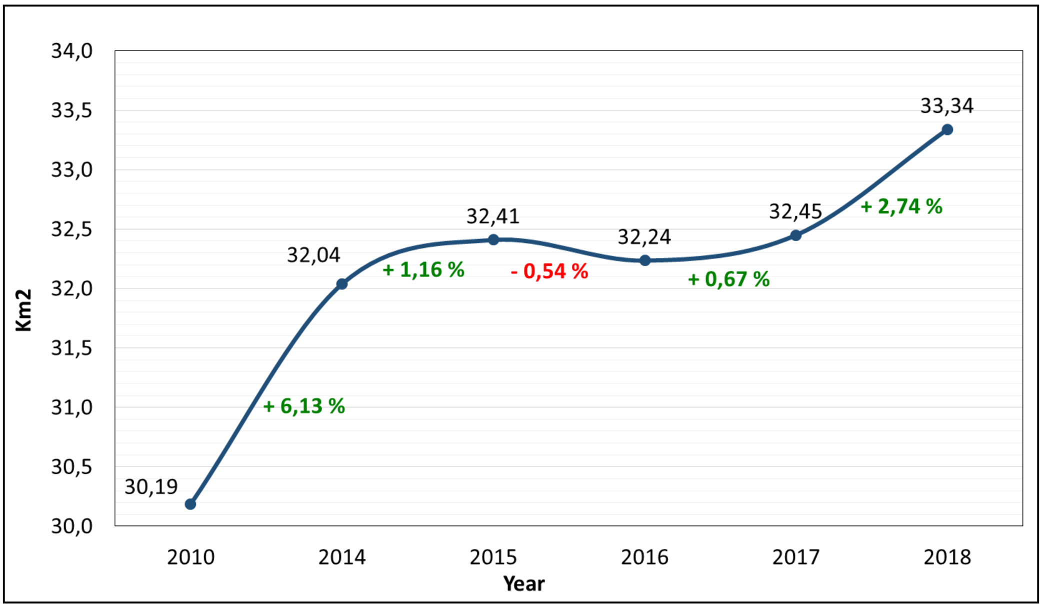

Figure 3. Area of water body changes 2010-2018

From the combinational observation of figures 2 and 3, it is understood that the area of the lake increases over time. More specifically, the highest growth rate is found during the first years after the reconstitution of the lake (2010-2014) with an increase of 6.13% (1.85 Km^2), while a negative change occurs between 2015 and 2016 with a 0.54% reduction in Lake area (0.17 Km^2). However, the change from 2010 to 2014 cannot be taken into account because it is not an annual change. As it is more clearly shown in Figure 4, the positive change is mainly located in the south part of Lake Karla while the most sides of the reservoir have not changed due to the infrastructure which is constructed to limit the lake's area. It has to be mentioned that at the sides of the constructions, small changes are noticed, related either to the angle of the image acquisition of the sensors (Thematic Mapper of Landsat 5 and C-SAR of Sentinel 1) or the water level changes.

Moreover, it is evident that the changes in the internal surface of the lake are related to the loss of land patches when the water level rises. This interaction is possibly related with the refill of the underground water supply due to the fact that this refill results in the expose of land patches and constructions like demarcation walls of parcels or roads created during the drying of the lake. In addition, it is worth noticing that the three artificial bird islets, located in the north of the lake, exhibit a fixed area over time, which is desirable for the biotope restoration.

With regard to Figure 5, concerning the monthly 2018 changes in the area of the lake using optical and SAR imagery, it is observed that the general course of variations does not follow a defined pattern, but common trends are identified. Generally, optical imagery attributes a larger area to the lake. More specifically, in March there is a common increase in the area, which is followed by a reduction in both cases.

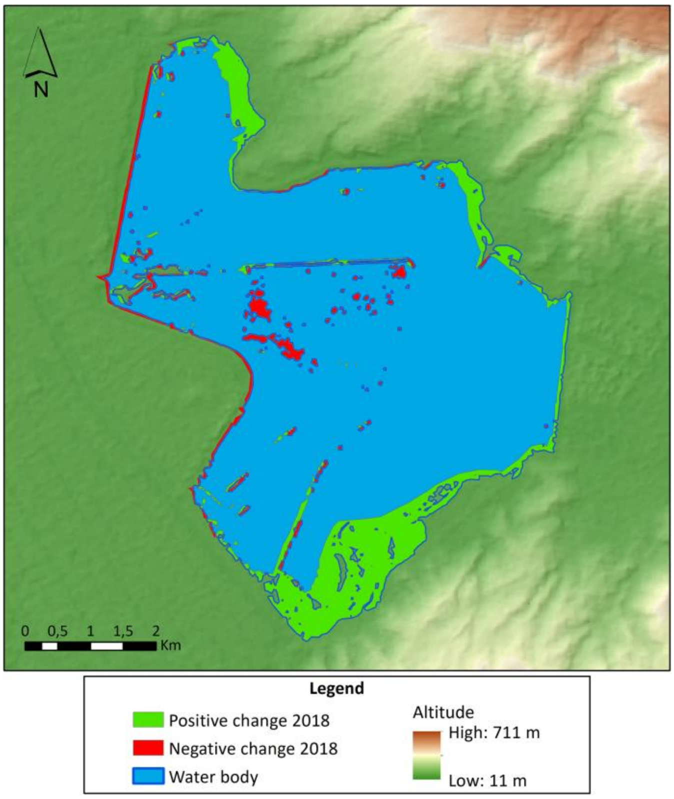

Figure 4. Annual area of water body changes 2010-2018 symmetrical difference.

For optical imagery between April-September, there are no strong fluctuations, which does not apply in the case of SAR. Between the two methods, the smallest difference in the lake's area is in July, while the largest in May. At this point, it should be noted that for November and December it was not possible to find images to complete the optical data set. The fluctuation is mostly related to the precipitation of each month and the agricultural irrigation period with the SAR to follow more accurately this relationship.

On the basis of the seasonal area comparison for 2017-2018 presented in Fig. 6, it is obvious that a relatively common course is followed, with an appearance of lower areas in June, possibly due to irrigation. In both years the precipitation plays an important role as it can be compared with the meteorological data.

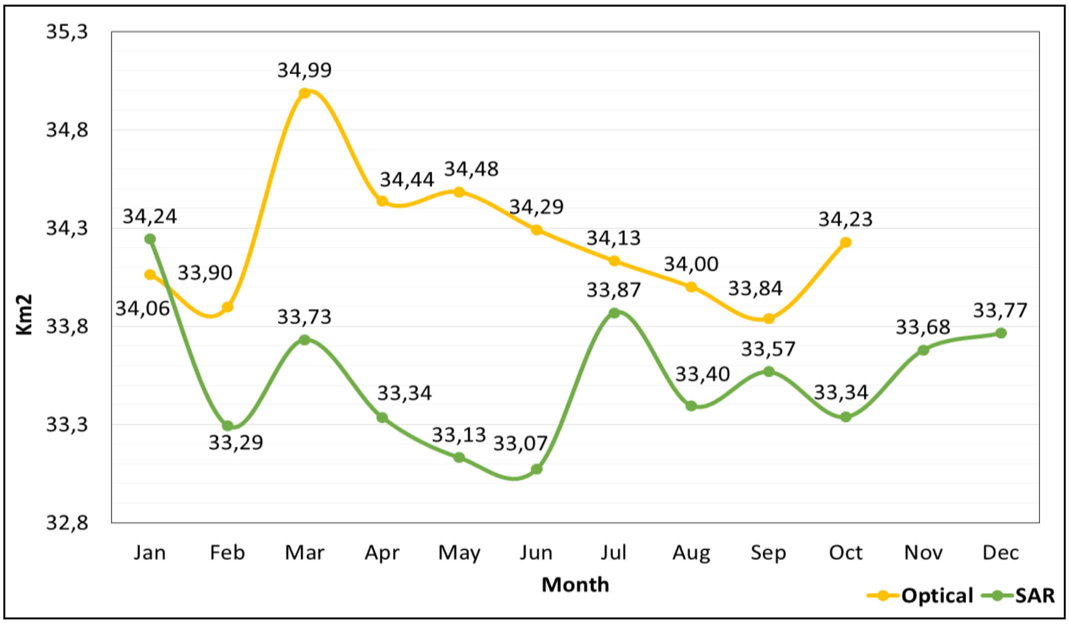

Figure 5. Area of water body changes per month optical and SAR comparison in 2018.

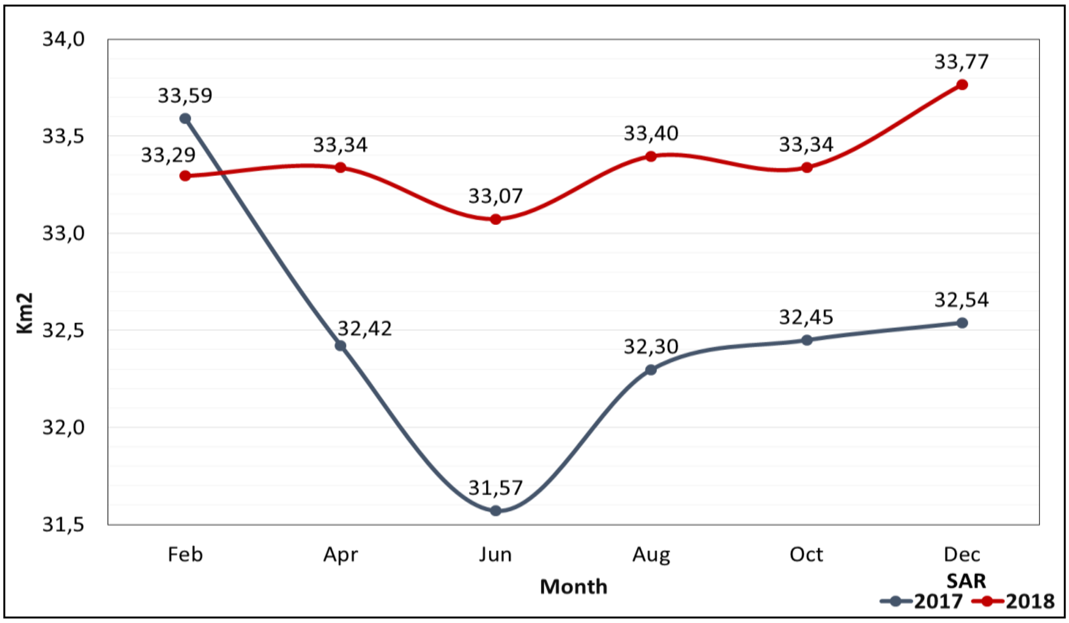

Figure 6. Area of water body changes per two months in 2017 and 2018.

5. DISCUSSION

Locating the temporal and spatial change patterns in a timeline, utilizing RS data and different methods, allows one to effectively monitor the variations of an inland water body. One suggestion for the expansion of the current work is the acquisition of measurements from the management body of Lake Karla, in order to validate the findings and decide which method suits better for the observation of inland water ecosystems.

Despite their benefits, RS data are accompanied with some limitations. RS data availability due to meteorological conditions, such as cloud coverage, is limited regarding optical sensors, thus not enabling us to assess the interval years between 2010-2014 period. Moreover, the RS data volume is high enough to require for the proper execution of the processing, in combination with the needed software, computing infrastructure of high performance. Regarding SAR imagery in inland water mapping, the polarization plays an important role because differences between the results of VV and VH polarizations are noticeable according to previous research. In addition, in cases of significant water level change or flooded areas, the use of averaging backscatter values of SAR imagery is more representative. Lastly, a decisive factor for the area estimation is the spatial and temporal resolution.

The rate of the reservoir area increase is low, maybe due to the high hydro permeable lake bed. This bed helped the refill of the underground water supply in this area utilizing the lake’s water. After the refill of the underground water supply, the rate of increase quickened as a result of some key factors like surface runoff and precipitation. It is important to be mentioned that the current Karla has less than half of the original natural lake acreage, making visible the different dynamics and benefits.

6. CONCLUSIONS

This study reached some conclusions. Regarding the imagery of different types utilized in the current study, optical imagery assigns a larger area to the lake than SAR imagery. It is suggested that a more thorough future research including validation of the results with the real state should be carried out. By combining the findings of the present work with rainfall data for the counter-temporal periods, it can be observed that the seasonal and monthly fluctuation of the lake area is basically due to rainfall and irrigation purposes. The artificial lake Karla may vary considerably from the natural lake that was dried in 1962, however, is a fairly important aquatic body for the broader area. In addition, on the basis of the results of this work, it seems that the objectives of the original design of the lake have been achieved greatly thus resolving the problems that the drainage caused. Taking into account what is previously mentioned, this study concludes that both RS data types are capable of sufficiently monitoring an inland water body but due to limitations of optical, SAR imagery can provide a more complete dataset for this purpose. Also, the importance of the remote sensing in inland waterbody monitoring it was proved again, like in similar studies, constituting a powerful cost-effective tool for this purpose. Lake area is basically due to rainfall and irrigation purposes. The artificial lake Karla may vary considerably from the natural lake that was dried in 1962, however, is a fairly important aquatic body for the broader area. In addition, on the basis of the results of this work, it seems that the objectives of the original design of the lake have been achieved greatly. Taking into account what is previously mentioned, this study concludes that both RS data types are capable of sufficiently monitoring an inland water body but due to environmental limitations of optical, SAR imagery can provide a more complete dataset for this purpose.

ACKNOWLEDGEMENTS

This study was accomplished during our studies in the Postgraduate Program "Applied Geography and Spatial Planning" at the Department of Geography of Harokopio University of Athens. For this reason, we would like to thank Dr. Issaak Parcharidis for his valuable guidance and encouragement for our first steps in scientific research.

REFERENCES

Bioresita, F., & Hayati, N. (2016). Coastline changes detection using sentinel-1 satellite imagery in Surabaya, east java, Indonesia. Geoid, 11(2), 190-198. DOI: 10.12962/j24423998.v11i2.1265.

Brisco, B. (2015), "Mapping and monitoring surface water and wetlands with synthetic aperture radar", in: Tiner, R. W., Lang, M. W., and Klemas, V. V. (eds.), RS of Wetlands: Applications and Advances, Boca Raton: CRC Press, pp. 119-136.

Climate Change Impacts Study Committee (2011). Impacts of climate change on the surface and underground water bodies of Greece, Athens: Bank of Greece. Retrieved from: https://www.itia.ntua.gr/el/getfile/1285/2/documents/Stournaras.pdf.

Corine Land Cover 2018 (2019). Copernicus Programme: Land Monitoring Service. Retrieved from: https://land.copernicus.eu/pan-european/corine-land-cover/clc2018.

Dellepiane, S., De Laurentiis, R., & Giordano, F. (2004). Coastline extraction from SAR images and a method for the evaluation of the coastline precision. Pattern Recognition Letters, 25(13), 1461-1470. https://doi.org/10.1016/j.patrec.2004.05.022.

European Space Agency, (2012).Sentinel-1 ESA's Radar Observatory Mission for GMES Operational Services, The Netherlands: ESA Communications. Retrieved from: https://sentinel.esa.int/documents/247904/349449/S1_SP-1322_1.pdf.

European Space Agency, (2012). Sentinel-2 Optical High-Resolution Mission for GMES Operational Services, The Netherlands: ESA Communications. Retrieved from: https://sentinel.esa.int/documents/247904/349490/S2_SP-1322_2.pdf.

European Space Agency, (2015). Sentinel-2 User Handbook. Retrieved from: https://sentinel.esa.int/documents/247904/685211/Sentinel-2_User_Handbook.

European Space Agency, (2019). Sentinel-1. Retrieved from: https://sentinel.esa.int/web/sentinel/missions/sentinel-1.

European Space Agency, (2019). Sentinel-2. Retrieved from: https://sentinel.esa.int/web/sentinel/missions/sentinel-2.

Gaki-Papanastassiou K. (2011). Quaternary evolution of the Agia-Agiokambos area as a possible outlet of the Eastern Thessaly plain to the Aegean Sea. Hellenic Journal of Geosciences, vol. 45, 101-108. Retrieved from: http://www.hellenjgeosci.geol.uoa.gr/45/Gaki-Papanastassiou.pdf.

Gerakis, P. (1992). Conservation and management of Greek wetlands, IUCN, Gland. Retrieved from: https://portals.iucn.org/library/sites/library/files/documents/WTL-002.pdf.

Lee, J. & Jurkevich, L. & Dewaele, Piet & Wambacq, Patrick & Oosterlinck, A.. (1994). Speckle filtering of synthetic aperture radar images: A Review. RS Reviews. 8. Doi: 10.1080/02757259409532206.

Liu, H., & Jezek, K. C. (2004). Automated extraction of coastline from satellite imagery by integrating Canny edge detection and locally adaptive thresholding methods. International journal of RS, 25(5), 937-958. https://doi.org/10.1080/0143116031000139890.

Liu, C. (2016). Analysis of Sentinel-1 SAR data for mapping standing water in the Twente region. Master Thesis, University of Twente, Faculty of Geo-Information Science and Earth Observation. Retrieved from https://webapps.itc.utwente.nl/librarywww/papers_2016/msc/wrem/cliu.pdf.

McFeeters, S. K. (1996). The use of the Normalized Difference Water Index (NDWI) in the delineation of open water features. International journal of RS, 17(7), 1425-1432. https://doi.org/10.1080/01431169608948714.

McFeeters, S. (2013). Using the normalized difference water index (NDWI) within a geographic information system to detect swimming pools for mosquito abatement: A practical approach. RS, 5(7), 3544-3561. https://doi.org/10.3390/rs5073544.

Ministry for the Environment, Spatial Planning and Public Works (2008). Reconstitution of Lake Karla: Project details file. Retrieved from: https://www.ypethe.gr/sites/default/files/basicpagefiles/2008_11_ypehode_stoiheia_ergoy_karlas.pdf.

Zormpas, K., Vasilakos, C., Athanasis, N., Soulakellis, N., & Kalabokidis, K. (2018). Dead fuel moisture content estimation using remote sensing. *European Journal of Geography*, 8(5), 17-32

Paes R. L., Nunziata F.& Migliaccio M., (2015) "Coastline extraction and coastal area classification via SAR hybrid-polarimetry architecture" 2015 IEEE International Geoscience and RS Symposium (IGARSS), Milan, 2015, pp. 3798-3801. doi: 10.1109/IGARSS.2015.7326651.

Parcharidis, I., (2015). Principles of satellite RS. [ebook] Athens: Hellenic Academic Libraries Link. Available Online at: http://hdl.handle.net/11419/3960 [In Greek].

Pradhan B., Rizeei H.M. & Abdulle A., (2018), Quantitative Assessment for Detection and Monitoring of Coastline Dynamics with Temporal RADARSAT Images. Remote Sens. 2018, 10, 1705. Retrieved from: https://doi.org/10.3390/rs10111705.

Prasad, N. R., Garg, V., & Thakur, P. K. (2018). ROLE OF SAR DATA IN WATER BODY MAPPING AND RESERVOIR SEDIMENTATION ASSESSMENT. SPRS Ann. Photogramm. Remote Sens. Spatial Inf. Sci., IV-5, 151-158. https://doi.org/10.5194/isprs-annals-IV-5-151-2018.

Sheng G., Yang W., Deng X., He C., Cao Y. & Sun H. (2012), Coastline Detection in Synthetic Aperture Radar (SAR) Images by Integrating Watershed Transformation and Controllable Gradient Vector Flow (GVF) Snake Model, IEEE Journal of Oceanic Engineering, vol. 37, no. 3, pp. 375-383. doi: 10.1109/JOE.2012.2191998.

Sidiropoulos P., (2014). Underground Water Resources Management under Uncertainty: The value of information on environmentally degraded aquifers, PhD Thesis, University of Thessaly, Department of Civil Engineering. Retrieved from: http://ir.lib.uth.gr/handle/11615/44623.

SNAP (2019). Calibration help.

USGS (2019). Landsat Missions Landsat 5. Retrieved from: https://www.usgs.gov/land-resources/nli/landsat/landsat-5?qt-science_support_page_related_con=0#qt-science_support_page_related_con.

Xenarios, S., Alamanos, A., Mylopoulos, N., & Stalnaacke, P. (2016). Hydro-economic modeling and management with limited data: the case of Lake Karla Basin. European Water, (54), 3. Retrieved from: https://research.nu.edu.kz/en/publications/hydro-economic-modeling-and-management-with-limited-data-the-case.

Xu, H. (2006). Modification of normalised difference water index (NDWI) to enhance open water features in remotely sensed imagery. International journal of RS, 27(14), 3025-3033. Retrieved from: https://doi.org/10.1080/01431160600589179.

Yu, Y., & Acton, S. T. (2002). Speckle reducing anisotropic diffusion. IEEE Transactions on image processing, 11(11), 1260-1270. DOI: 10.1109/TIP.2002.804276.

Zisou C. & Psilovikos A., (2012). Monitoring and assessment of the water quality in newly newly established Lake Karla. Paper presented at the 3rd Panhellenic Planning and Regional Development Conference, Volos, Greece, Retrieved from: https://www.researchgate.net/publication/320445078_PARAKOLOUTHESE_KAI_E_APOTIMESE_TES_POIOTETAS_TON_YATON_STE_NEOSYSTATHEISA_LIMNE_KARLA [in Greek].

Water Resources and Environment of Thessaly (2019). Tribute to Lake Karla. Retrieved from: https://www.ypethe.gr/archive/afieroma-sti-limni-karla-periehomena-arheia [in Greek].

